REVISTA MATÉRIA V.30
ISSN 1517-7076 articles e20240847, 2025

Effect of element Nb and V alloying on austenite grain growth behavior in 45Mn5Al4 steel

Xin Yaxuan[1], Ding Haisen[2], Guo Qiang[2], Guo Fanghui[1], Li Junru[1]

[1]Qingdao University, College of Mechanical and Electrical Engineering. 266071, Qingdao, China.

[2]Rizhao Ruixin Machinery Manufacture Co., Ltd. 267800, Rizhao, China.

e-mail: 15092160211@163.com, 13066080388@163.com, guo13346330827@163.com, guofanghui_qdu@163.com, lijunru_qdu@163.com

ABSTRACT

A new martensitic low-density steel was designed, and the behavior of austenite grain growth, along with the influence of niobium Nb and V microalloying, was investigated. The results indicated that the austenite grain growth rate in the new martensitic low-density steel was rapid, the austenite grains gradually increased in size with rising austenitizing temperatures, reaching a coarsening temperature of approximately 1000°C. Nb microalloying significantly refined the austenite grain structure and elevated the coarsening temperature to about 1200°C. Nb microalloying resulted in the formation of two size ranges of NbC precipitates: those smaller than 0.3 μm and those larger than 2 μm. The formation of NbC precipitates was the primary reason for the reduced grain growth rate in the Nb microalloyed experimental steel. The NbC precipitate phase hindered the migration of austenite grain boundaries, thereby slowing down the grain growth rate. The NbC precipitates smaller than 0.3 μm dissolved in large quantities when heated above 1200°C, weakening the nailing effect on grain boundaries, which was the main reason for the rapid grain growth observed in the experimental steel. Conversely, the NbC precipitates larger than 2 μm were difficult to eliminate, even when subjected to prolonged heating at 1250°C. The austenite grain growth model for the newly designed martensitic low-density steel was calculated as: $D = 1.47 \times 10^3 \cdot t^{0.097} \cdot e^{-52423/RT}$, (900–1150°C) $D = 3.45 \times 10^{14} \cdot t^{0.108} \cdot e^{-367331/RT}$, (1200–1250°C).

Keywords: Low-density steel; Grain growth; NbC precipitates; Dissolution.

1. INTRODUCTION

In recent years, the automobile industry has seen an increasing demand for lightweight materials [1–3], making high-strength steel a promising candidate for body structural components due to its exceptional strength and formability [4, 5]. This type of steel can contribute to a lighter and safer vehicle body. Fe-Al-Mn-C low-density steel, recognized as the third generation of high-strength steel, is particularly valued for its low density and high strength, positioning it as a favorable material for automotive applications [6]. The high aluminum content in this steel leads to lattice expansion by decreasing the average molar mass of the material, which in turn reduces the mass density of the steel [7, 8]. Current research on Fe-Mn-Al-C low-density steel primarily focuses on low-density steel plates, with insufficient attention given to low-density steel bars. This paper investigates a novel type of martensitic low-density steel, 45Mn5Al4, with the aim of its application in automotive bars. The research and application of this steel are significant for advancing the lightweight design of automobiles.

In recent years, the application of microalloying elements in high-strength steels has become a focal point of research [9]. For instance, XIE *et al.* [10] investigated the effects of annealing temperature and vanadium addition on Fe-Mn-Al-C low-density steel, finding that the incorporation of vanadium refines the grain structure and enhances the strength and hardness of the material. SUN *et al.* [11] demonstrated that Nb and V microbial loys effectively refine the recrystallized grains, significantly improving high-temperature plasticity. The addition of Nb, V, Ti, and other strong carbonitride-forming elements can produce fine carbonitride precipitates, resulting in a precipitation-strengthening effect that enhances the properties of steel. Among these elements, Ti (C, N) exhibits high stability and dissolves at elevated temperatures, effectively pinning grain boundaries to inhibit grain growth [12]. Similarly, Nb (C, N) can impede the recrystallization process, refine the grains, and also dissolve at high temperatures [13]. The dissolved Nb atoms may be solubilized in austenite,

Corresponding Author: Li Junru Received on 28/11/2024 Accepted on 12/03/2025

DOI: https://doi.org/10.1590/1517-7076-RMAT-2024-0847

influencing the stability of austenite and the subsequent phase transition process. Additionally, when V (C, N) is heated to a specific temperature and dissolved, it may re-precipitate during the subsequent cooling process, contributing to the precipitation-strengthening effect [10]. Collectively, these mechanisms highlight the critical role of carbonitride-forming elements in optimizing the microstructure and mechanical properties of steel.

In addition, structural design and process optimization are essential strategies for enhancing the performance of low-density steel.Among these strategies, the refinement of austenite grains is particularly crucial for the performance of high-strength steels [14]. YANG *et al.* [15] investigated the refinement and isothermal growth behavior of austenite grains in low-carbon vanadium micro-alloyed steels and found that the addition of vanadium effectively inhibits the growth of austenite grains, thereby refining the final microstructure. YUAN *et al.* [16] discovered that as the austenite grains are refined, the ferrite transformation temperature increases during cooling, resulting in a higher ferrite content in the microstructure after cooling. AKHTAR and KHAJURIA [17] examined the impact of the original austenite grain size in boron-modified P91 steel on the microstructure and creep properties of the simulated heat-affected zone. They found that fine austenite grains can significantly enhance the creep resistance of the material.

Consequently, this paper examines the grain growth behavior of 45Mn5Al4 steel and elucidates the influence mechanisms of microalloying elements and their precipitation on austenite grain growth behavior. In particular, it focuses on the effects of different sizes of niobium carbide precipitates, providing a theoretical foundation for optimizing the heat treatment process and microalloying design.

2. MATERIALS AND METHODS

The chemical composition of the experimental steel is presented in Table 1. The test steel was forged into a φ130 mm bar after melting. The initial forging temperature was 1150°C, while the final forging temperature was 900°C. Subsequently, the steel was annealed at 700°C for 1 hour.

The experimental steel was cut to dimensions of 8 mm × 8 mm × 12 mm using wire cutting. The samples were divided into Group A and Group B. Group A samples were utilized to study austenite grains, while Group B samples were used to investigate precipitated phases. To examine the effect of heating temperature on grain growth, two groups of experimental steel, A and B, were heated and maintained at various temperatures (950, 1000, 1050, 1100, 1150, 1200, and 1250 °C) for 30 minutes in a box heating furnace. Group A samples were rapidly cooled to 600 °C and held for 90 minutes before being water-cooled to room temperature. This method enabled the researchers to observe the grain boundaries of austenite clearly. After quench-ing, Group B samples were directly cooled with water to room temperature to prevent oxidation.

Following quenching, the samples from Group A were cut in half, polished, and then subjected to electrolytic corrosion. The corrosion reagent used was a 2% oxalic acid solution, with a current intensity of 0.15 A, and the corrosion process lasted for 30 seconds at room temperature to reveal the original austenite grain boundaries. The samples from Group B were also cut in half after quenching, polished, and then etched with nitrate alcohol to observe the microstructure and precipitated phases.

In order to investigate the effect of holding time on grain growth, the experimental steel was maintained at various temperatures (950, 1000, 1050, 1100, 1150, 1200, and 1250 °C) for different durations (15 min, 30 min, 90 min, 120 min). Subsequently, the original austenite grains were examined using optical microscopy. The average grain size was measured using Nano Measurer software. The microstructure of the test steel was analyzed with a scanning electron microscope (SEM), while the precipitated phases were studied using a transmission electron microscope (TEM). The chemical composition of the precipitated phases was analyzed using an energy-dispersive spectrometer (EDS). The carbon film replica method was employed to extract the precipitated phases from the experimental steel for TEM analysis.

3. RESULTS

3.1. Original microstructure observation

Figure 1 illustrates the original structure of the two experimental steels. It is evident that both steels contain a significant number of precipitates, with an average size ranging from 0.3 to 1.5 μm, uniformly distributed throughout the matrix. The 45Mn5Al4VNb steel exhibited additional precipitates, with sizes not exceeding 0.3 μm and not smaller than 2 μm.

The results of the EDS analysis of the precipitates, along with the TEM morphology and diffractograms, are presented in Figure 2. EDS analysis was conducted on the MC depicted in Figure 1(c), with the results presented in Figure 2(a). Additionally, EDS analysis was performed on NbC depicted in Figure 1(c); the results for point 2 are displayed in Figure 2(b), while the results for point 3 are presented in Figure 2(c).

Table 1: Chemical composition of 45Mn5Al4 steel (in mass%).

STEEL	C	Al	Mn	Si	P	S	Cr	V	Nb	Fe
45Mn5Al4	0.44	3.62	5.14	0.45	0.025	0.003	0.11	—	—	Bal.
45Mn5Al4VNb	0.45	3.38	5.07	0.48	0.03	0.003	0.11	0.13	0.09	Bal.

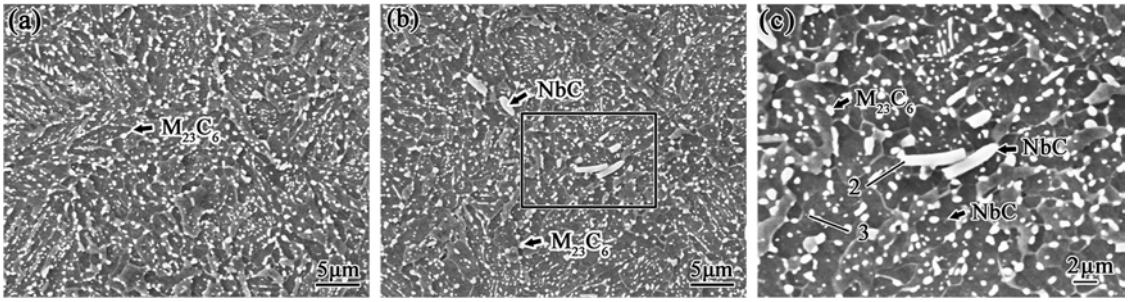

Figure 1: SEM images of the original microstructure of the experimental steel. (a) 45Mn5Al4 steel, (b)(c) 45Mn5Al4VNb steel.

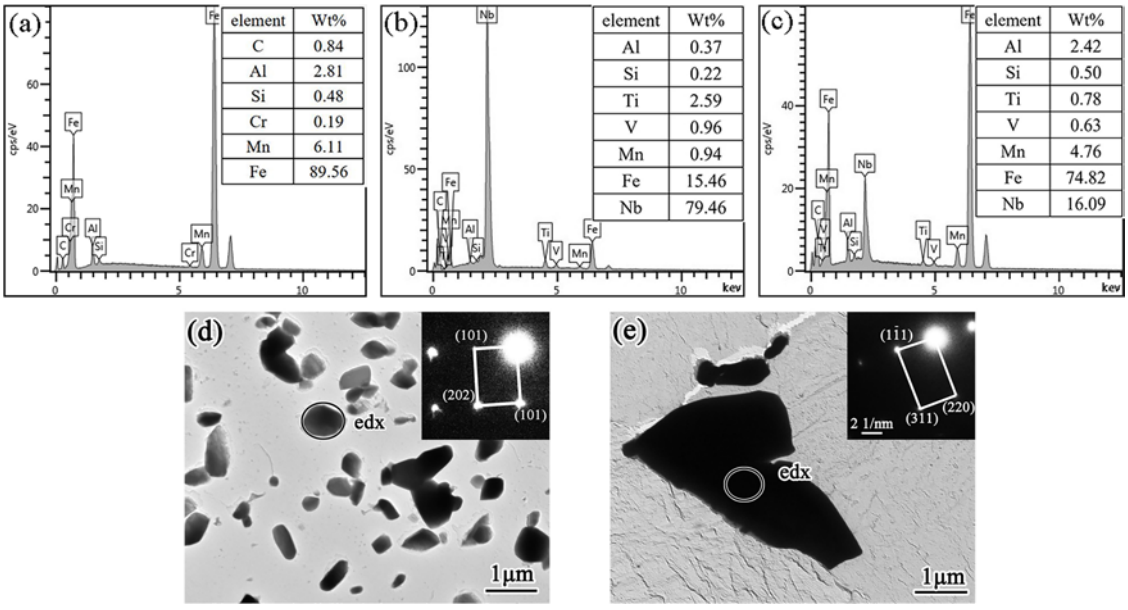

Figure 2: EDS analysis results of precipitates. (a) size 0.3~1.5 μm, (b) size no smaller than 2 μm, (c) size no larger than 0.3 μm. and TEM image of the precipitates. (d) size 0.3~1.5 μm, (e) size no smaller than 2 μm.

The EDS results indicate that the Fe and Mn elements are present in greater quantities in the precipitates measuring 0.3 to 1.5 μm, while the diffractogram calibration results confirm that these are M23C6 precipitates, as shown in Figures 2(a) and 2(d). In 45Mn5Al4 steel, both small and large precipitates are identified as NbC precipitates. The small precipitates typically have a diameter of less than 0.3 μm, while the large precipitates have diameters greater than 2 μm. The distribution and morphology of these precipitates are clearly illustrated in Figures 2(b), 2(c), and 2(e).

Generally, the size of small precipitates is less than 0.3 microns, while the diameter of large precipitates exceeds 2 microns, as illustrated in Figures 2(b), (c), and (e).

3.2. Austenite grain growth behavior

The austenite grain diagrams of the experimental steel at various heating temperatures are presented in Figures 3 and 4. It is evident that the grain size increases with rising heating temperatures. The grain growth of 45Mn5Al4 steel occurs rapidly. In contrast, the grain size of 45Mn5Al4VNb steel remains fine at temperatures ranging from 900 to 1200°C. However, at 1250°C, the austenite grains exhibit significant coarsening. Abnormal growth of austenite grains in both 45Mn5Al4 steel and 45Mn5Al4VNb steel is observed at 950°C and 1150°C, respectively.

Figure 5 illustrates the average austenite grain size of the experimental steel at various heating temperatures and holding times. It is evident that the grain growth rate increases with rising heating temperatures and remains relatively stable with prolonged holding times, indicating that holding time has minimal effect. This phenomenon can be attributed to thermodynamic and kinetic factors. Higher temperatures provide atoms with increased energy, which accelerates diffusion. Diffusion is a critical mechanism for grain growth, as it enables atoms to migrate across grain boundaries, leading to the enlargement of larger grains at the expense of smaller ones, thereby promoting grain growth. After extended holding periods, grain growth primarily occurs at the grain boundaries. The reduction in boundary area limits the sites available for atomic diffusion, resulting in the stabilization of the grain growth rate [18].

The austenitic grain size of 45Mn5Al4 steel exhibits a linear increase. In contrast, the austenitic grain size of 45Mn5Al4VNb steel grows slowly between 900°C and 1200°C but accelerates at 1250°C. Notably, at the same temperature, the austenitic grain size of 45Mn5Al4VNb steel is larger than that of 45Mn5Al4 steel.

3.3. Analysis phase observation

Figures 6(a) and 6(b) illustrate the microstructure of the experimental steel at 950°C, while Figure 6(e) presents the TEM morphology and diffraction patterns of the precipitated phase in 45Mn5Al4VNb. In 45Mn5Al4 steel, M23C6 and NbC precipitates were completely dissolved. In 45Mn5Al4VNb steel, the M23C6 precipitated phase was entirely dissolved in the matrix at 950°C, while the NbC precipitated phase retained its integrity, showing no significant dissolution. These NbC precipitates stabilize the austenitic grain boundaries, thereby refining the grains and significantly reducing the grain size of 45Mn5Al4VNb steel [19], which is notably smaller than that of 45Mn5Al4 steel without the addition of the Nb element [15].

Figure 6(c) and Figure 6(d) depict the microstructure of 45Mn5Al4VNb steel at 1200°C and 1250°C. Compared to the images, it is evident that the number of precipitates smaller than 3 microns at 1200°C was significantly reduced compared to that at 950°C. Consequently, NbC precipitates with a particle size of no more than 0.3 μm remain dissolved at 1200°C. This size of NbC particles can effectively inhibit the migration

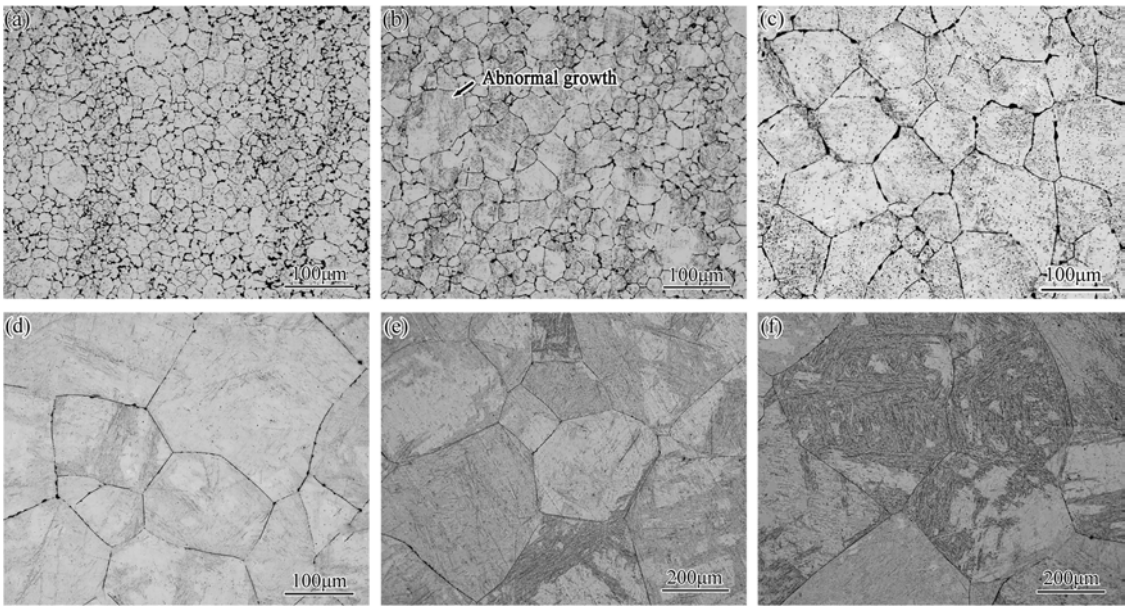

Figure 3: Morphology of austenite grains of the 45Mn5Al4 steel at different heating temperatures for 30 min, (a) 900°C, (b) 950°C, (c) 1000°C, (d) 1050°C, (e) 1100°C, (f) 1150°C.

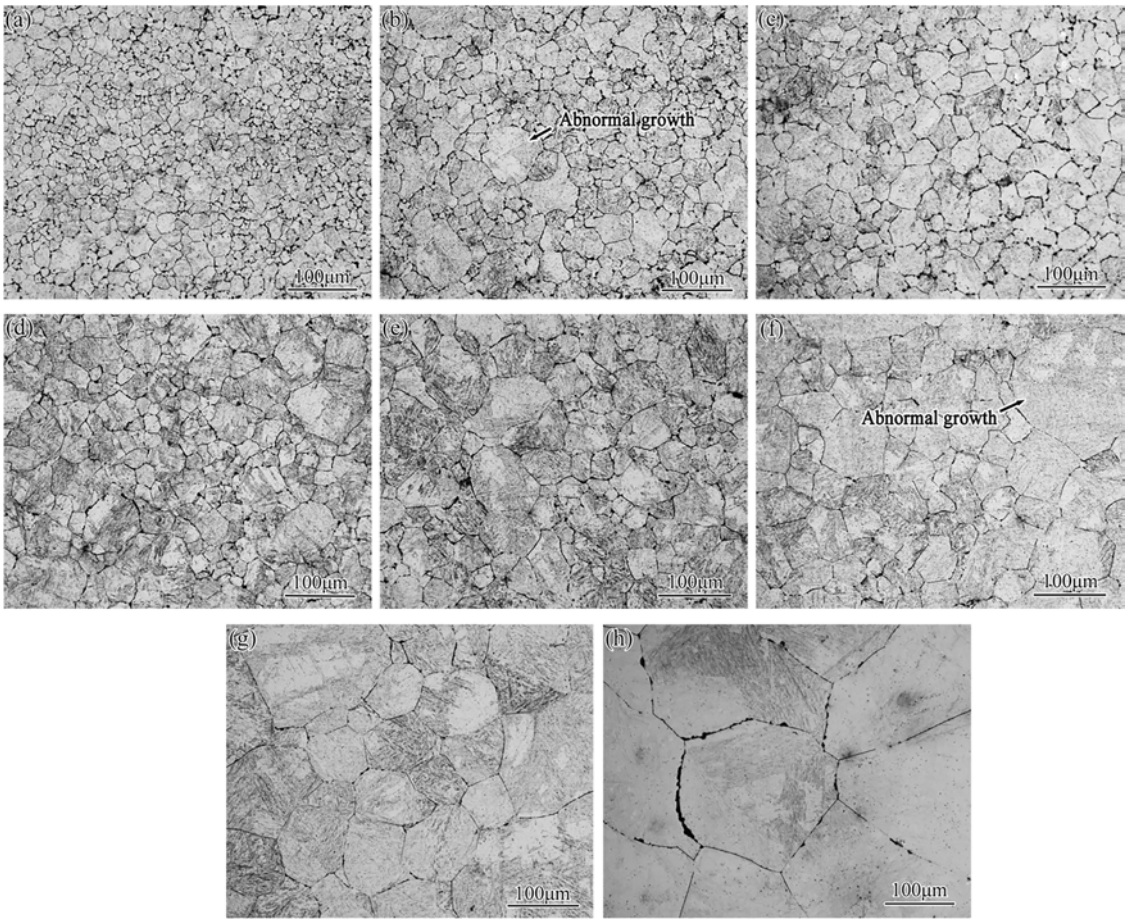

Figure 4: Morphology of austenite grains of the 45Mn5Al4VNb steel at different heating temperatures for 30 min. (a) 900°C, (b) 950°C, (c) 1000°C, (d) 1050°C, (e) 1100°C, (f) 1150°C, (g) 1200°C, (h) 1250°C.

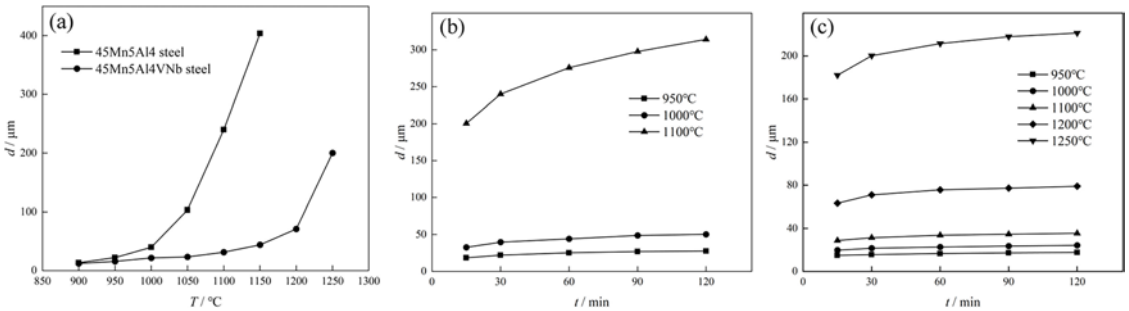

Figure 5: Average austenite grain size at different heating temperatures(a) and average austenite grain size at different holding times. (b) 45Mn5Al4 steel, (c) 45Mn5Al4VNb steel.

of grain boundary elements, allowing the steel to form fine austenite grains at a heating temperature of 1200°C. However, it is observed that NbC precipitates with sizes no larger than 0.3 μm dissolve at 1250°C, leading to a significant decrease in the pinning force of NbC particles. Consequently, the austenite grains can escape the inhibition of NbC and grow rapidly.

The NbC precipitates were usually nanoscale, but there were NbC precipitates larger than 2 μm in the 45Mn5Al4VNb steel. These larger NbC precipitates were likely formed during the smelting process, which can adversely affect the mechanical properties of the steel, particularly its toughness [20, 21]. It was observed that the NbC precipitates remained difficult to eliminate even after 12 hours at 1250°C, as shown in Figure 7.

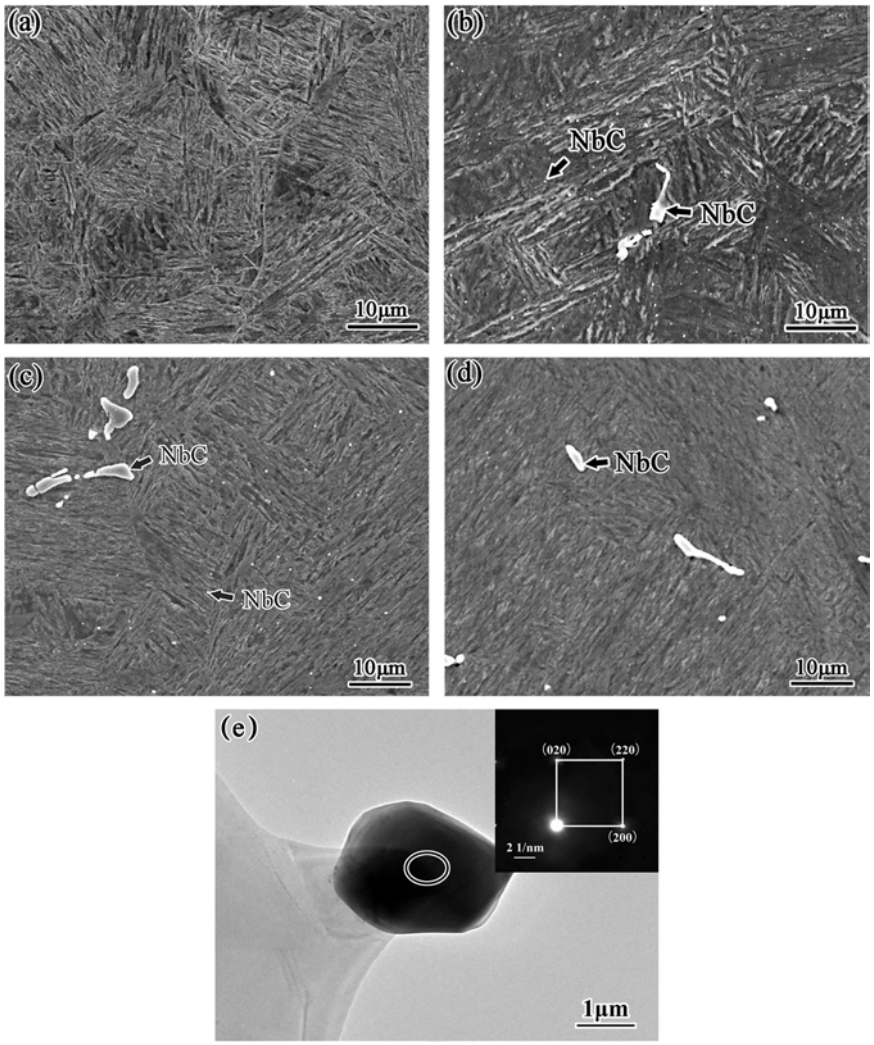

Figure 6: SEM image of the experimental steel after holding at 950 °C for 30 min. (a) 45Mn5Al4 steel, (b) 45Mn5Al4VNb steel. and SEM images of the 45Mn5Al4VNb steel after holding at different temperatures for 30 min. (a) 1200°C, (b) 1250°C, and (e) TEM image of the precipitates.

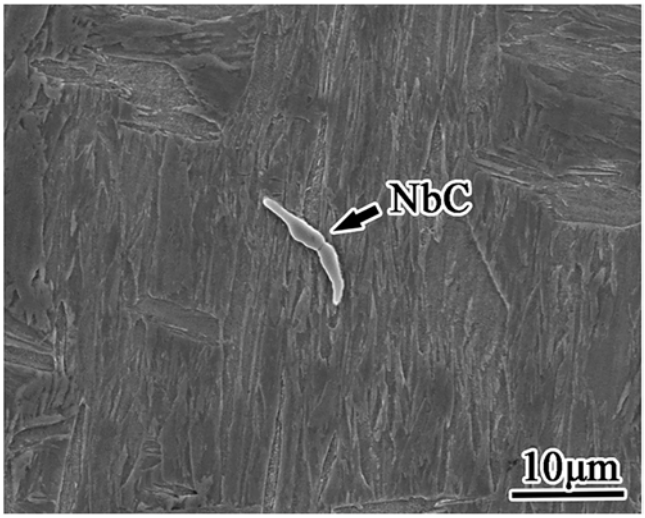

Figure 7: Large-size niobium carbides after heating for 12 h at 1250°C.

The temperature required for the complete dissolution of NbC precipitates is influenced by the concentrations of Nb and C [22], and the solubility product can be expressed by Equation (1):

$$\log K_s = \log[Nb]\,[C] = A - B/T \tag{1}$$

A and B are constants, K_s is the equilibrium constant, [*Nb*] is the mass fraction of dissolution Nb (wt%), [*C*] is the dissolution amount of C (wt%), and *T* is the absolute temperature (K). The constants A and B are not fixed; they are influenced by various factors, including the experimental conditions, the materials under investigation, and the specific thermodynamic model employed.

It can be observed from Equation (1) that the complete dissolution temperature of NbC precipitates increases with higher C and Nb content. The 45Mn5Al4VNb steels contain up to 0.6% carbon and 0.08% niobium, leading to elevated complete dissolution temperatures of NbC precipitates. When designing the composition of medium- and high-carbon steels, it is essential to control the niobium content to prevent the formation of large NbC precipitates.

3.4. Mathematical model of austenite grain growth

From the analysis above, heating temperature and holding time are two critical factors influencing austenite grain growth behavior. To thoroughly investigate the austenite grain growth in the experimental steel, both the heating temperature (T) and holding time (t) must be taken into account.

At present, the mathematical model commonly used for predicting austenite grain size during isothermal processes is the Arrhenius model [23], as represented by the following equation (2):

$$D = A \cdot t^n \cdot \exp\,(-Q/RT) \tag{2}$$

Where *D* is the average austenite grain size after coarsening, μm; *t* is the holding time, s; *T* is the heating temperature, K; *R* is the molar gas constant, J/(mol·K); *Q* is the activation energy of grain growth; *A*, *n* and *B* are experimental parameters.

By logarithmic transformation of equation (2), equation (3) is derived:

$$ln\,D = lnA + nlnt - Q/RT \tag{3}$$

When the heating temperature was held constant, the fitted relationship of lnD versus lnt was obtained, as shown in Figure 8. Based on this curve, the grain growth index (n) can be calculated, where n represents the index of the grain growth rate. The grain growth indices for 45Mn5Al4 steel were 0.194, 0.205, and 0.214 at temperatures of 950°C, 1000°C, and 1100°C, respectively. In contrast, the grain growth indices for 45Mn5Al4VNb steel were 0.082, 0.095, 0.100, 0.108, and 0.111 at 950°C, 1000°C, 1100°C, and 1250°C, respectively.

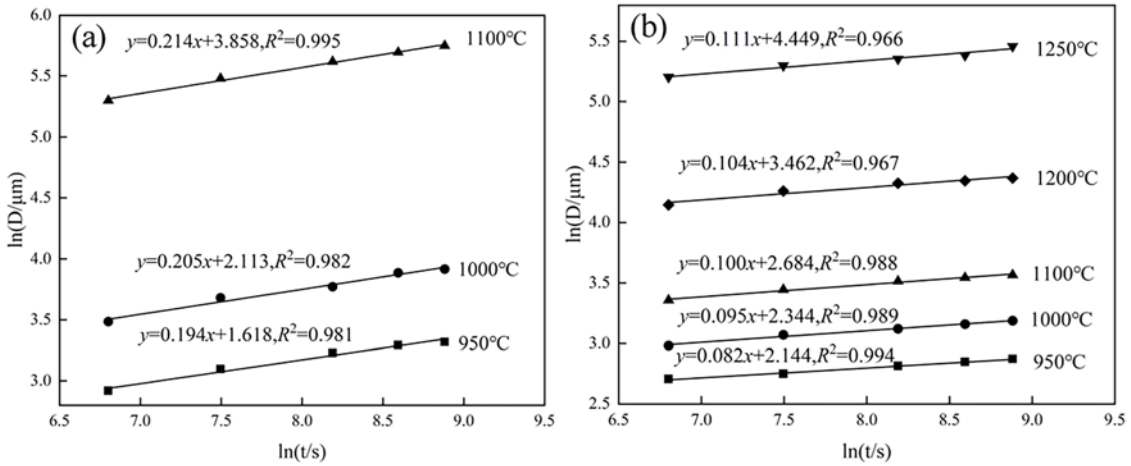

Figure 8: lnD-lnt curves of experimental steel in the process of isothermal austenitization. (a) 45Mn5Al4 steel, (b) 45Mn5Al4VNb steel.

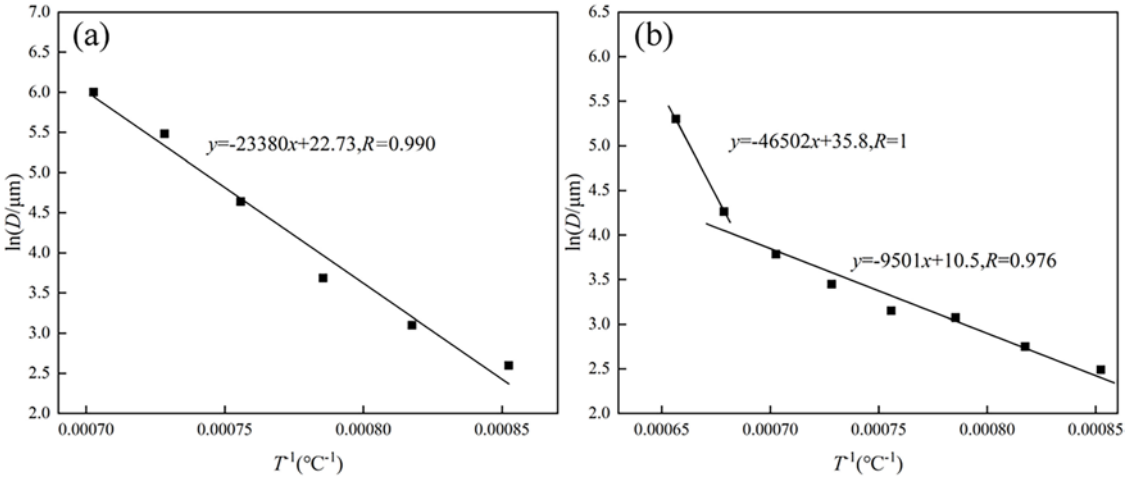

Figure 9: lnD-1/T curve of experimental steel in the process of heating. (a) 45Mn5Al4 steel, (b) 45Mn5Al4VNb steel.

When holding time constant, the fitted relationship curve of lnD-T^{-1} was shown in Figure 9, from which the grain boundary activation energy (Q) can be obtained.

The activation energy Q in 45Mn5Al4 steel was measured at $208695 J \cdot mol^{-1}$ and lnA was 22.16. In contrast, the activation energy Q in 45Mn5Al4VNb steel were $52423 J \cdot mol^{-1}$ and $367311 J \cdot mol^{-1}$ from 900°C to 1200°C and above 1200°C, respectively, and the lnA at 900°C to 1200°C and above 1200°C was 7.29 and 33.47. The grain growth models for 45Mn5Al4 steel and 45Mn5Al4VNb steel, both below and above the grain coarsening temperature, are presented in equations (4), (5), and (6).

$$D = 4.21 \times 10^{9} \cdot t^{0.204} \cdot e^{-208695/RT} \text{ (45Mn5Al4 steel)} \quad (4)$$

$$D = 1.47 \times 10^{3} \cdot t^{0.097} \cdot e^{-52423/RT} \text{ (45Mn5Al4VNb steel (900–1150°C))} \quad (5)$$

$$D = 3.45 \times 10^{14} \cdot t^{0.108} \cdot e^{-367331/RT} \text{ (45Mn5Al4VNb steel (1200–1250°C))} \quad (6)$$

The predicted grain size values were derived from the mathematical model, while the measured values are presented in Figure 10. The experimental results demonstrated a strong correlation with the predicted values, exhibiting relative deviations of 8.8% for 45Mn5Al4 steel and 7.7% for 45Mn5Al4VNb steel. Consequently, the model holds significant reference value.

4. CONCLUSIONS

From the investigation of Nb microalloying in the new martenstic low-density steel, the following conclusions were drawn:

(1) In the temperature range of 900–1100°C, the austenite grains of 45Mn5Al4 steel exhibited a linear increase. In the range of 900–1200°C, the austenite grain growth of 45Mn5Al4VNb steel was relatively slow; however, at a temperature of 1250°C, the austenite grains of 45Mn5Al4VNb steel underwent significant coarsening. This phenomenon can be attributed to the substantial dissolution of NbC precipitates in 45Mn5Al4VNb steel, which were no larger than 0.3 μm. The dissolution weakened the pinning effect, leading to a marked increase in grain size.

(2) The experimental steel was annealed with a significant amount of M23C6-type precipitates, which ranged in size from 0.3 to 1.5 μm and dissolved at 950°C. The 45Mn5Al4VNb steel contained additional NbC precipitates, which were no larger than 0.3 μm and no smaller than 2 μm. The NbC precipitates measuring no larger than 0.3 μm dissolved at 1250°C, while those measuring no smaller than 2 μm remained difficult to dissolve even after 12 hours at 1250°C.

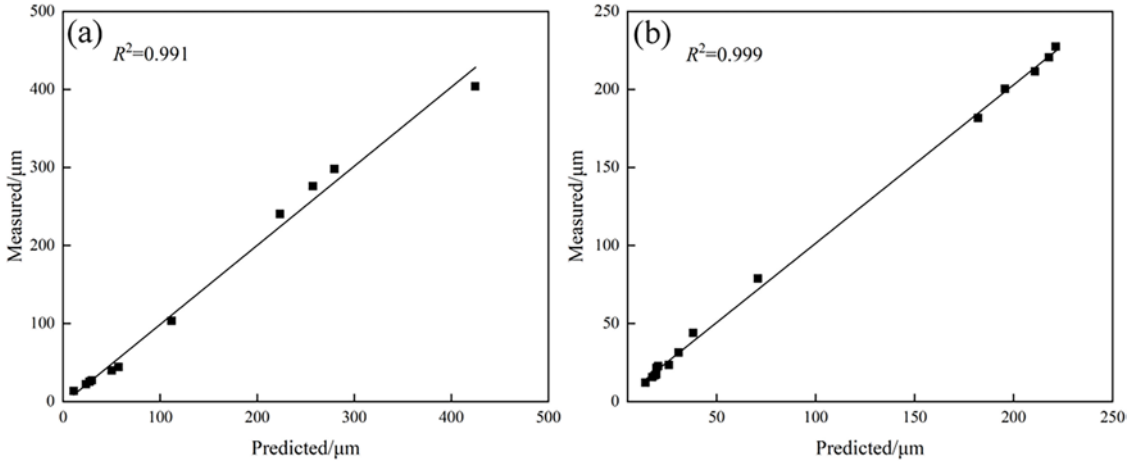

Figure 10: Correlation between experimental and predicted grain size values. (a) 45Mn5Al4 steel, (b) 45Mn5Al4VNb steel.

(3) The kinetic model for austenite growth of experimental steel were constructed:

$$D = 4.21 \times 10^{9} \cdot t^{0.204} \cdot e^{-208695/RT} \text{ (45Mn5Al4 steel)}$$

$$D = 1.47 \times 10^{3} \cdot t^{0.097} \cdot e^{-52423/RT} \text{ (45Mn5Al4NbV steel, 900–1150°C)}$$

$$D = 3.45 \times 10^{14} \cdot t^{0.108} \cdot e^{-367331/RT} \text{ (45Mn5Al4NbV steel, 1200–1250°C)}$$

5. ACKNOWLEDGMENTS

This work was supported by the National Natural Science Foundation of China (No. 51701100) and the Supported by China Postdoctoral Science Foundation (No. 2020T130552) and the Science and Technology Support Plan for Youth Innovation of Colleges in Shandong Province (No. DC2000000891).

6. BIBLIOGRAPHY

[1] ZHANG, W., XU, J., "Advanced lightweight materials for automobiles: a review", *Materials & Design*, v. 221, pp. 110994, Sep. 2022. doi: http://doi.org/10.1016/j.matdes.2022.110994.

[2] TRZEPIECINSKI, T., NAJM, S.M., "Current trends in metallic materials for body panels and structural members used in the automotive industry", *Materials (Basel)*, v. 17, n. 3, pp. 590, Feb. 2024. doi: http://doi.org/10.3390/ma17030590. PubMed PMID: 38591480.

[3] NINA, B., DRAGAN, A., NENAD, G., *et al*., "Lightweight materials for automobiles", *IOP Conference Series. Materials Science and Engineering*, v. 1271, n. 1, pp. 012010, 2022. doi: http://doi.org/10.1088/1757-899X/1271/1/012010.

[4] LIU, Q., ZHENG, X., ZHANG, R., *et al*., "Medium manganese high strength steel for automotive application: status quo and prospects", *Materials Review*, v. 33, n. 4A, pp. 1215–1220, 2019.

[5] ZHAO, Z., CHEN, W., GAO, P., *et al*., "Progress and perspective of advanced high strength automotive steel", *Journal of Iron and Steel Research*, v. 32, n. 12, pp. 1059–1076, 2020.

[6] CHEN, S.P., RANA, R., HALDAR, A., *et al.*, "Current state of Fe-Mn-Al-C low density steels", *Progress in Materials Science*, v. 89, pp. 345–91, Aug. 2017. doi: http://doi.org/10.1016/j.pmatsci.2017.05.002

[7] PRAMANIK, S., SUWAS, S., "Low-density steels: the effect of Al addition on microstructure and properties", *Journal of the Minerals Metals & Materials Society*, v. 66, n. 9, pp. 1868–1876, 2014. doi: http://doi.org/10.1007/s11837-014-1129-2.

[8] RAABE, D., SPRINGER, H., GUTIERREZ-URRUTIA, I., *et al*., "Alloy design, combinatorial synthesis, and microstructure-property relations for low-density Fe-Mn-Al-C austenitic steels", *Journal of the*

Minerals Metals & Materials Society, v. 66, n. 9, pp. 1845–1856, Sep. 2014. doi: http://doi.org/10.1007/s11837-014-1032-x.

[9] WANG, S.Z., GAO, Z.J., WU, G.L., *et al*., "Titanium microalloying of steel: a review of its effects on processing, microstructure and mechanical properties", *International Journal of Minerals Metallurgy and Materials*, v. 29, n. 4, pp. 645–661, Apr. 2022. doi: http://doi.org/10.1007/s12613-021-2399-7.

[10] XIE, Z.Q., HUI, W.J., BAI, S.Y.H., *et al.*, "Effects of annealing temperature and V Addition on microstructure and mechanical properties of Fe-Mn-Al-C austenitic low-density steel", *Materials Today Communications*, v. 35, pp. 14, Jun. 2023. doi: http://doi.org/10.1016/j.mtcomm.2023.106328

[11] SUN, C., LI, X.Q., GUO, F.H., *et al*., "Effects of Nb and V microalloying on the thermoplasticity of new martensitic low-density steels", *Matéria (Rio de Janeiro)*, v. 28, n. 3, pp. e20230214, 2023. doi: http://doi.org/10.1590/1517-7076-rmat-2023-0214.

[12] MA, H., LIAO, S.L., WANG, S.F., "Effect of Ti on austenite grain growth behavior in high carbon steels", *Journal of Iron and Steel Research International*, v. 21, n. 7, pp. 702–709, Jul. 2014. doi: http://doi.org/10.1016/S1006-706X(14)60109-6.

[13] ANNAN, K.A., SIYASIYA, C.W., STUMPF, W.E., "Austenite grain growth kinetics after isothermal deformation in microalloyed steels with varying Nb concentrations", *ISIJ International*, v. 58, n. 2, pp. 333–339, 2018. doi: http://doi.org/10.2355/isijinternational.ISIJINT-2017-464.

[14] LI, X.C., LU, G.Y., WANG, Q.C., *et al*., "The effects of prior austenite grain refinement on strength and toughness of high-strength low-alloy steel", *Metals*, v. 12, n. 1, pp. 28, Jan. 2022. doi: http://doi.org/10.3390/met12010028.

[15] YANG, G.W., SUN, X.J., YONG, Q.L., *et al*., "Austenite grain refinement and isothermal growth behavior in a low carbon vanadium microalloyed steel", *Journal of Iron and Steel Research International*, v. 21, n. 8, pp. 757–764, Aug. 2014. doi: http://doi.org/10.1016/S1006-706X(14)60138-2.

[16] YUAN, X., YAN, X.Q., LI, J.R., *et al*., "Study on the relationship between process organization and properties of 45mnvs non-tempered steel", *Matéria (Rio de Janeiro)*, v. 29, n. 2, pp. e20230316, 2024. doi: http://doi.org/10.1590/1517-7076-rmat-2023-0316.

[17] AKHTAR, M., KHAJURIA, A., "Effects of prior austenite grain size on impression creep and microstructure in simulated heat affected zones of boron modified P91 steels", *Materials Chemistry and Physics*, v. 249, pp. 13, Jul. 2020. doi: http://doi.org/10.1016/j.matchemphys.2020.122847

[18] PU, E.X., LIU, M., ZHENG, W.J., *et al*., "Investigation on behavior of grain growth in superaustenitic stainless steel 654smo", *Journal of Materials Engineering and Performance*, v. 24, n. 10, pp. 3897–3904, Oct. 2015. doi: http://doi.org/10.1007/s11665-015-1654-3.

[19] FU, L.M., WANG, H.R., WANG, W., *et al*., "Austenite grain growth prediction coupling with drag and pinning effects in low carbon Nb microalloyed steels", *Materials Science and Technology*, v. 27, n. 6, pp. 996–1001, Jun. 2011. doi: http://doi.org/10.1179/1743284711Y.0000000001.

[20] LI, J.R., HE, T., ZHANG, P.F., *et al*., "Effect of large-size carbides on the anisotropy of mechanical properties in 11cr-3co-3w martensitic heat-resistant steel for turbine high temperature blades in ultra-supercritical power plants", *Materials Characterization*, v. 159, pp. 9, Jan. 2020. doi: http://doi.org/10.1016/j.matchar.2019.110025.

[21] LI, X.G., CAI, Z.P., HU, M.J., *et al.*, "Effect of Nbc precipitation on toughness of X12crmownbvn10-1-1 martensitic heat resistant steel for steam turbine blade", *Journal of Materials Research and Technology*, v. 11, pp. 2092–2105, Mar-Apr. 2021. doi: http://doi.org/10.1016/j.jmrt.2021.02.049

[22] PALMIERE, E.J., GARCIA, C.I., DEARDO, A.J., "Compositional and microstructural changes which attend reheating and grain coarsening in steels containing niobium", *Metallurgical and Materials Transactions. A, Physical Metallurgy and Materials Science*, v. 25, n. 2, pp. 277–286, Feb. 1994. doi: http://doi.org/10.1007/BF02647973.

[23] RAZALI, M.K., ABD GHAWI, A.A., IRANI, M., *et al.*, "Practical approach for determining material parameters when predicting austenite grain growth under isothermal heat treatment", *Materials*, v. 16, n. 19, pp. 6583, Oct. 2023. doi: http://doi.org/10.3390/ma16196583